atmosphere

MDPI

Article

High Resolution Chemical Stratigraphies of Atmospheric Depositions from a 4 m Depth Snow Pit at Dome C (East Antarctica)

Laura Caiazzo [1,2], Silvia Becagli [2,3], Stefano Bertinetti [4], Marco Grotti [4,*], Silvia Nava [1,5], Mirko Severi [2,3] and Rita Traversi [2,3]

1 National Institute for Nuclear Physics (INFN)-Florence Division, 50019 Sesto Fiorentino, Italy; laura.caiazzo@unifi.it (L.C.); nava@fi.infn.it (S.N.)
2 Department of Chemistry "Ugo Schiff", University of Florence, 50019 Sesto Fiorentino, Italy; silvia.becagli@unifi.it (S.B.); mirko.severi@unifi.it (M.S.); rita.traversi@unifi.it (R.T.)
3 Institute of Polar Sciences, ISP-CNR, 30172 Venice-Mestre, Italy
4 Department of Chemistry and Industrial Chemistry, University of Genoa, 16146 Genoa, Italy; stefano.bertinetti@edu.unige.it
5 Department of Physics and Astronomy, University of Florence, 50019 Sesto Fiorentino, Italy
* Correspondence: grotti@unige.it

Abstract: In this work, we present chemical stratigraphies of two sampling lines collected within a 4 m depth snow pit dug in Dome C during the Antarctic summer Campaign 2017/2018, 12 years after the last reported snow pit. The first sampling line was analyzed for nine anionic and cationic species using Ion Chromatography (IC); the second sampling line was analyzed for seven major elements in an innovative way with Inductively Coupled Plasma Optical Emission Spectroscopy (ICP-OES) after sample pre-concentration, allowing the study of deposition processes of new markers especially related to crustal source. This coupled analysis, besides confirming previous studies, allowed us to investigate the depositions of the last decades at Dome C, enriching the number of the detected chemical markers, and yielding these two techniques complementary for the study of different markers in this kind of matrix. As a result of the dating, the snow layers analyzed covered the last 50 years of snow depositions. The assessment of the accumulation rate, estimated about 9 cm yr^{-1}, was accomplished only for the period 1992–2016, as the eruption of 1992 constituted the only tie-point found in $nssSO_4^{2-}$ depth profile. Na, the reliable sea salt marker, together with Mg and Sr, mainly arose from marine sources, whereas Ca, Al and Fe originated from crustal inputs. Post-depositional processes occurred on Cl^- as well as on NO_3^- and methanesulfonic acid (MSA); compared to the latter, Cl^- had a more gradual decrease, reporting a threshold at 2.5 m for the post-depositional process completion. For NO_3^- and MSA, instead, the threshold was shallower, at about 1 m depth, with a loss of 87% for NO_3^- and of 50% for MSA.

Keywords: dome C; snow pit; ion chromatography; ICP-OES; chemical stratigraphies; post-depositional processes; dating; primary aerosol

Citation: Caiazzo, L.; Becagli, S.; Bertinetti, S.; Grotti, M.; Nava, S.; Severi, M.; Traversi, R. High Resolution Chemical Stratigraphies of Atmospheric Depositions from a 4 m Depth Snow Pit at Dome C (East Antarctica). *Atmosphere* **2021**, *12*, 909. https://doi.org/10.3390/atmos12070909

Academic Editor: Paulo Artaxo

Received: 22 June 2021
Accepted: 12 July 2021
Published: 14 July 2021

1. Introduction

When considering future climate change, it is imperative to look at the record of climate variation in the past, which allows researchers to learn about the range of natural climate variability, compare it with predictive climatic models, and look for evidence of recent climate change due to humans' activities.

Permanently ice-covered regions of the world preserve the past composition of the Earth's atmosphere, since they incorporate trace quantities of water-soluble and insoluble elements. In particular, ice cores drilled in Antarctica represent valuable archives of paleo-climatic and paleo-environmental information [1,2]. During the past years, numerous ice cores have been drilled at several Antarctic sites, with different temporal resolutions

(e.g., [3–6]); however, many uncertainties still remain in specific aspects. For instance, the mechanisms which control air masses provenance, the transport process (including any possible fractionation phenomena of chemical species), the markers' seasonality, the depositional and post-depositional processes [3], the spatial variability in snow accumulation rate and chemical composition still remain as not fully explained aspects.

Thanks to its position on the top of a large dome with a minute slope, the absence of the typical intense katabatic wind [7], and the mean annual temperature of −54.5 °C [8], Dome C was chosen for a deep drilling down to bedrock, accomplished in the framework of EPICA (European Project for Ice Coring in Antarctica) in the 1996–2004 summer fields, which provided and still provides precious information about the last 800 kyrs' past climate (e.g., [1,3,9]), since it still represents the oldest ice core to date. Moreover, in the framework of the new project "Beyond EPICA—Oldest Ice", the international ice core community worked to find a new site for retrieving a continuous ice core going back 1.5 million years. The most suitable site for this purpose was identified 50 km far from Dome C [10]. Given the proximity between the two sites, studies on the aerosol transport and depositional processes in the inner plateau, and in particular, in Dome C, still play a fundamental role allowing the synchronization and calibration of the records of the new ice core, thus improving data interpretation.

Since the EPICA ice core did not cover the 6 m shallowest snow layers, during the 2000/01 Antarctic Campaign a 7 m depth snow pit was dug. Furthermore, in the 1997/98, 1998/99 and 2005/06 campaigns, three more snow pits were carried out around the Dome C area, aiming at contributing to a better interpretation of the EPICA stratigraphies and assessing the spatial variability in different points of the area [11].

Chemical stratigraphies from snow pits also provide fundamental information on current crustal/ocean/atmosphere/snow exchange mechanisms regarding atmospheric aerosol, transport processes, and the entity and frequency of depositional and post-depositional processes on the snow cover [12,13].

In this work, we present high-resolution chemical stratigraphies on a 4 m depth snow pit collected at the end of December 2017 (about 12 years later than the previous one), in the framework of the PNRA SIDDARTA project. This study gives the possibility to verify, complement, and increase our knowledge about the processes occurring in Dome C, providing a major understanding of the paleo-records from EPICA ice core.

For this purpose, nine ionic water-soluble compounds were determined by ion chromatographic analysis, namely Na^+, K^+, Mg^{2+}, Ca^{2+}, F^-, methanesulfonic acid (MSA), Cl^-, $NO_3{}^-$, $SO_4{}^{2-}$. Thus, we compared these stratigraphic records with those obtained from the previous snow pits, including the post-depositional processes involving certain ions and the assessment of the accumulation rate. In addition, seven major elements, Al, Ca, Fe, K, Mg, Na, and Sr, were analyzed by ICP-OES after sample pre-concentration.

Studies based on ion chromatography are well documented in the literature, and highlight high sensitivity, reproducibility, and suitability for analysis, measuring low concentrations of soluble ions in snow pit and ice/firn core samples, without sample pretreatment (e.g., [14,15]). Conversely, the elemental analysis of Antarctic snow by ICP-OES is rarely reported due to the extremely low analytical concentrations (from tens of pg g^{-1} for Sr to tens of ng g^{-1} for Na); more sophisticated instruments having higher sensitivity, such as ICP-MS, are usually used [16,17]. Recently, a new method based on ICP-OES, carrying out the simultaneous determination of major elements in Antarctic snow samples, has been developed and validated [18]. Fit-for-purpose performances have been obtained by combining a 100-fold samples pre-concentration procedure with a total consumption microsample introduction system to overcome the obstacles posed by the low analyte concentrations.

2. Sampling

The Italian–French Concordia Station (75°06′ S, 123°21′ E, elevation: 3233 m a.s.l.) is located on the East Antarctic plateau south of the Indian Ocean, 1100 km far from the sea.

The thickness of the ice cap is 3250 ± 25 m; the annual accumulation rate is less than 10 cm per year, as reported from snow surveys [19], and it is due to the extremely low humidity in the atmosphere [7].

A 4 m depth snow pit was dug 5 km far from Concordia Station in the clean area around the scientific base (geographic coordinates: 75°03′ S 123°34′ E; Figure 1), during the Antarctic summer Campaign 2017/2018. This site was chosen in order to avoid winds with direction coming from the station, which could cause contamination [20].

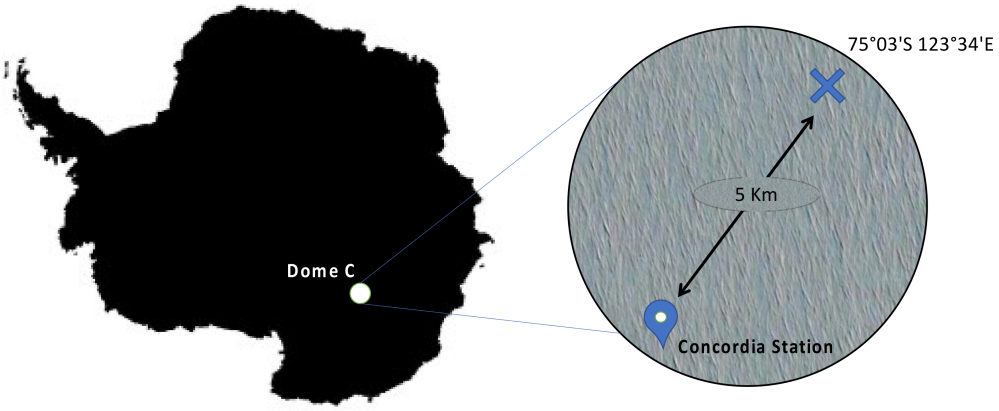

Figure 1. Map of Antarctica, indicating Dome C site (**left**). Point and GPS coordinates of the snow pit site, located 5 km far from Concordia Station (**right**).

The snow pit was dug by hand in order to avoid any kind of contamination and, before collecting samples, a sufficient snow layer was removed with a pre-cleaned polypropylene scraper [20]. The samples were collected at different depths using 2.4–3.0 cm diameter 50 mL polypropylene (PP) vials, which were only opened immediately before use in the snow pit. The vials were pushed into the snow pit wall one next to the other along a vertical line, so the sampling resolution is approximately the same as the vial diameter, from 2.5 to 3.1 cm.

In the same snow pit, 6 parallel lines of sampling were collected reaching a depth of 389.8 cm, to enable different kind of analysis.

All the samples were stored singularly in sealed polyethylene bags, labeled, and kept frozen in insulated box, and then transported to Italy. Once in Italy, they were preserved in the cold room at −20 °C.

3. Chemical Measurements

In this work, two lines of sampling from the snow pit were considered and analyzed using two different analytical methods.

The first method allowed analyzing anions (F^-, acetate, formate, MSA, Cl^-, NO_3^-, SO_4^{2-}) and cations (Na^+, NH_4^+, K^+, Mg^{2+}, Ca^{2+}) through a DX 500 and ICS1000 Thermo-Fisher Dionex conductivity-suppressed ion-chromatographic integrated system. Among these, ammonium, acetate, and formate ions will not be further considered, because of the large uncertainty due to multiple possibilities of contamination that may be occurred during sampling, sample handling, and analysis. The whole analysis procedure, from sample handling to the analytes' determination, was realized in the clean room located at the University of Florence (class 10,000). The samples were melted in a clean room under a class-100 laminar flow hood, still closed in their vials, and each sample was transferred into an individual accuvette. Then, the accuvettes were placed into a Gilson 222 XL liquid handler automated sampler. The use of such a sampler permitted to minimize the contamination risk by sample handling, since a stainless-steel needle drill through the accuvette plastic cap, aspires the liquid sample and injects it into the two Ion Chromatography (IC) systems by using a peristaltic pump [15,21]. For information about analytical performances and

detection limit, refer to [15]. In total, 111 samples were analyzed using this method, covering the total length of the snow pit.

The second method is based on the simultaneous determination of Al, Ca, Fe, K, Mg, Na and Sr through the Thermo Fisher Scientific (Waltham, MA, USA) iCAP 6300 Inductively Coupled Plasma Optical Emission Spectroscopy (ICP-OES) Duo instrument. This analysis was carried out in the laboratories of the University of Genoa. The snow samples were allowed to melt at room temperature still closed in their tubes, obtaining about 20 mL of water. Then, the samples were acidified in HNO_3 and HF 0.5% (v/w) and let to rest for 24 h. Afterwards they were freeze-dried and then the inner walls of the tubes were washed with 200 µL of a solution HNO_3 0.05% (v/v) to collect all the material remained after the lyophilization. Therefore, the samples volumes were reduced from about 20 mL to 200 µL, providing a 100-fold pre-concentration of the analytes. The amount of snow of each treated sample was obtained weighting the tubes before and after the freeze-dried process. The accuracy of the analytical method was verified by using the certified natural water SRM 1640a, supplied by NIST. The detailed procedure is provided in [18].

In this case, from the overall available samples, 59 were pre-processed and analyzed, chosen in order to uniformly cover the total length of the snow pit. The remanent snow samples will be used in further studies.

All reagents used in this work were ultrapure grade quality from Sigma-Aldrich, and all steps of the pre-concentration procedure were conducted under a laminar flow work area. The ICP-OES instrument used for this work is equipped with a total consumption microsample introduction system that allowed us to carry out the analysis of the seven analytes, consuming only the available 200 µL of sample [22–24].

At the best of our knowledge, this is the first time that this procedure was used to analyze trace metals in snow samples at such low concentrations with ICP-OES.

4. Results and Discussion

Table 1 reports median, mean, and standard deviation of all chemical components analyzed.

Table 1. Median, mean (both expressed in ng g^{-1}) and standard deviation of every component analyzed. For each of them, the analytical method used is specified.

Element	Analytical Method	Median (ng g^{-1})	Mean (ng g^{-1})	Std Dev
Al	ICP-OES	0.68	1.16	1.82
Ca	ICP-OES	2.64	3.21	2.44
Fe	ICP-OES	0.76	1.09	0.98
K	ICP-OES	1.54	1.75	1.05
Mg	ICP-OES	2.53	2.61	1.17
Na	ICP-OES	17.00	17.21	8.08
Sr	ICP-OES	0.022	0.023	0.010
Na^+	IC	19.91	20.73	10.40
K^+	IC	1.09	1.50	1.25
Mg^{2+}	IC	2.61	2.61	0.89
Ca^{2+}	IC	2.86	3.43	2.22
Cl^-	IC	60.61	66.24	33.37
NO_3^-	IC	12.58	25.70	29.55
SO_4^{2-}	IC	83.28	86.38	27.79
MSA	IC	8.26	9.39	5.05

The number of samples analyzed by ICP-OES is less than those analyzed by IC. In any case, they have been chosen to cover the entire length of the snow pit, and thus, to have representative information regarding the element trends along the entire depth.

Four elements, namely sodium, potassium, magnesium, and calcium, were analyzed using both techniques. Their comparison of mean values from Table 1 results in a good agreement, as visible in the IC/ICP ratio: 1.20 for sodium, 0.86 for potassium, 1.0 for magnesium, and 1.06 for calcium (Table 2). However, these results belong to different number of samples analyzed (111 samples analyzed by IC versus 58 samples analyzed by ICP-OEC). Since the two series were collected in parallel within the same pit, with a lateral distance between 30 and 40 cm, we may consider the snow at the same depth as isotropic on a horizontal plane. Therefore, it is possible identifying a selection of 58 pared series' samples (i.e., the samples having exactly the same depth); considering this correlation, we recalculated the IC/ICP ratio (Table 2), and we made a regression analysis (Table 3).

Table 2. IC/ICP ratio of the mean values for the four elements analyzed with IC and ICP-OES techniques. In brackets, the numbers of the samples considered for each technique are specified.

Element	Na	K	Mg	Ca
IC/ICP (111/58)	1.20	0.86	1.00	1.06
IC/ICP (58/58)	1.11	0.71	1.00	1.11

Table 3. Slopes (±error) and Pearson's correlation coefficients for the four elements analyzed by both techniques, namely sodium, potassium, magnesium and calcium. Correlations are all significant ($p < 0.01$, $n = 58$).

Element	Na	K	Mg	Ca
Slope (±error)	1.07 ± 0.05	0.72 ± 0.10	0.85 ± 0.04	0.68 ± 0.09
Correlation coefficient	0.93	0.68	0.93	0.72

The slopes, reported in Table 3, and shown in Figure S1, highlight that, for K and Ca in particular, the acid pre-treatment of the pre-concentration process used before ICP-OES analysis can dissolve some insoluble particles in water, not detectable by IC [25]. Moreover, the high temperature of ICP allows also the insoluble particles present in the sample solution to be atomized. In part, this effect is also detectable for Mg.

Regarding sodium, instead, the slope around 1.00 indicates how IC and ICP-OES tend to solubilize the same amount of particles.

These preliminary results were determined through an innovative procedure making use of ICP-OES for the analyses of snow samples. They furthermore highlighted the complementarity of both analytical techniques for the study of principal and trace markers in ice cores.

4.1. Sea Salt-Non-Sea Salt Contributions

In central Antarctica, studies on ice cores showed that, although Na^+ mainly arises from marine sources, part of Na^+ can also derive from crustal sources. Similarly, Ca^{2+}, which mainly derives from continental dust, can also have marine origins [26,27]. For this reason, in order to quantitively take into account these two different contributions, the following system of Equations (1)–(4) was used to calculate the sea salt (ss) and non-sea salt (nss) fraction of Na^+ and Ca^{2+}:

$$totNa^+ = ssNa^+ + nssNa^+ \quad (1)$$

$$totCa^{2+} = ssCa^{2+} + nssCa^{2+} \quad (2)$$

$$ssNa^+ = totNa^+ - 0.562\ nssCa^{2+} \quad (3)$$

$$nssCa^{2+} = totCa^{2+} - 0.038\ ssNa^+ \quad (4)$$

where 0.562 = Na^+/Ca^{2+} (w/w) in the crust [28], and 0.038 = Ca^{2+}/Na^+ (w/w) in seawater [29].

Consistent with previous studies [11,27,30], the sea salt fraction of Na^+ which reaches Dome C is always dominant. Indeed, $ssNa^+$ represents (as an average percentage) 92.6% of total Na^+ (Figure 2—top). Even if with a lower number of samples, similarly, ssNa analyzed by ICP-OES results in an average percentage at 91.5% of total Na. This is due both to the relatively lower importance of extra sea salt sources and to the lack of fractionating phenomena occurring during transport, even in the increasing of altitude and distance from the coast [31].

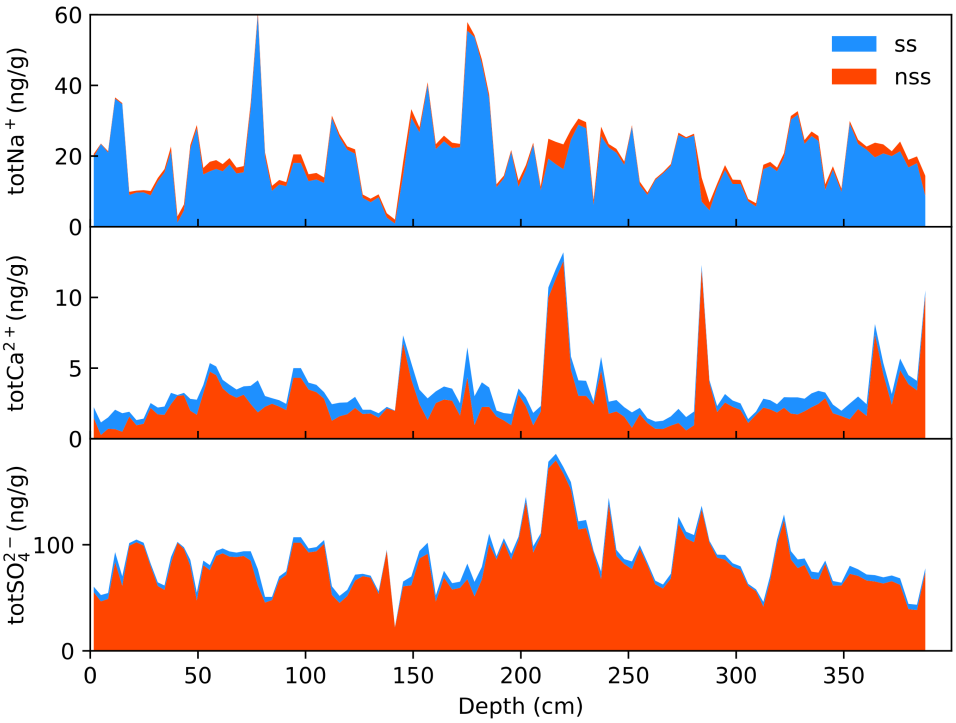

Figure 2. Sodium (**top**), calcium (**middle**) and sulphate (**bottom**) concentration vs. depth profiles. The total measured sodium, calcium and sulphate are shown as the sum of the two different contributions: sea salt (in light blue), and non-sea salt (in red).

To this extent, the use of sodium as univocal marker for sea spray is confirmed by several works [26,27,30,32].

Conversely to Na, Ca sea salt/non-sea salt profile (Figure 2—middle) shows an extremely high percentage of non-sea salt contribution, with an average percentage of 80.0%, in accordance to what was found in the older snow pits. The same mean percentage was found for calcium analyzed by ICP-OES. Changes in $nssCa^{2+}$ concentration, reflecting changes in the atmospheric load of mineral dust, can be interpreted as changes in atmospheric transport from dust source areas, different lifetimes of dust in the atmosphere due to different wet scavenging efficiency during the transport, or changes in dust source areas' climatic conditions.

As was done for sodium, we will not correct calcium concentrations, as the percentages of ssCa are nearly negligible.

To better distinguish the different sources also for the ions, which are particularly relevant as aerosol source and/or transport processes, in particular, SO_4^{2-}, both the sea salt and the non-sea salt fraction were calculated by means of the following Equation (5):

$$nssSO_4^{2-} = SO_4^{2-} - 0.253\ ssNa^+ \quad (5)$$

where $0.253 = SO_4^{2-}/Na^+$ (w/w) in the seawater [28].

In this way, it was possible to assess the different contributions of primary marine sources from secondary sulphate aerosol (biogenic and volcanic). Figure 2 (bottom) shows the total SO_4^{2-} concentration, taking into account the two different contributions. The non-sea salt percentage is extremely high: 93.9% of the total sulphate budget, confirming the dominant contribution of secondary sources to the total sulphate at Dome C. This result is perfectly consistent with the available literature [33,34], in which was observed that the percentage of $nssSO_4^{2-}$ is the lowest at stations near the sea and increases progressively with the distance from the sea.

4.2. Dating

The dating of a snow pit is fundamental for accurately understanding climate records and comparing with other records from snow pits collected in a different time and place, in order to study the temporal and spatial variability of climatic and environmental variations.

At Dome C, a stratigraphic dating based on summer and winter layer identification cannot be gained; this because annual snow precipitation is extremely low, ranging between 2.8 and 3.7 g cm^{-2} yr^{-1} (corresponding to 8–8.8 cm of snow yr^{-1}) as water equivalent in the period 1964–1992 [11]. In fact, the sampling resolution mentioned above (2.5–3.3 cm) provides at maximum only three to four samples per year, precluding to identify any seasonal patterns. Thus, a correct dating and, consequently, a mean accumulation rate evaluation, was accomplished using individual historically recorded events which are usually observed in the concentration vs. depth profiles as clear peaks superimposed over a natural and sometimes seasonal background. These emissions could range from natural events (e.g., explosive volcanic eruption) to mankind-related ones (e.g., nuclear tests) and are historically known, such as those that can potentially be used as a tie-point in the dating [35].

Following a major explosive eruption, intense emissions of gaseous sulphur compounds in the atmosphere such as SO_2 and H_2S occur, later oxidized to a fine aerosol of H_2SO_4 [36]. As a result, sudden increases in the concentration of H_2SO_4 or SO_4^{2-} in polar snow are usually observed during a short period (0–3 years) immediately after the eruptive phenomenon [37].

In order to achieve a temporal frame for the analyzed snow pit samples and an estimation of the accumulation rate, we relied on the $nssSO_4^{2-}$ concentration profile, as done by [11]. Our data (field season 2017/2018) were compared with SO_4^{2-} concentration profiles from snow pit samples collected in previous campaigns, namely 1997/1998, 1998/1999, 2000/2001 and 2005/2006. These four profiles (see Figure 3 in [11]) show two outstanding concentration peaks that have been associated with specific volcanic eruptions recorded into the firn. In particular, the oldest signal was ascribed to the eruptions of Mount Agung (Indonesia, 1963). The two more recent volcanic events, instead, corresponded to the eruption of Mount Pinatubo (Luzon, Philippines, June 1991), with the sulphate deposition occurred in mid-1992–mid-1994, and the eruption of Cerro Hudson (Chile, August 1991), having higher preexisted spike due to the deposition of volcanic aerosol traceable to late 1991–mid-1992 period [37].

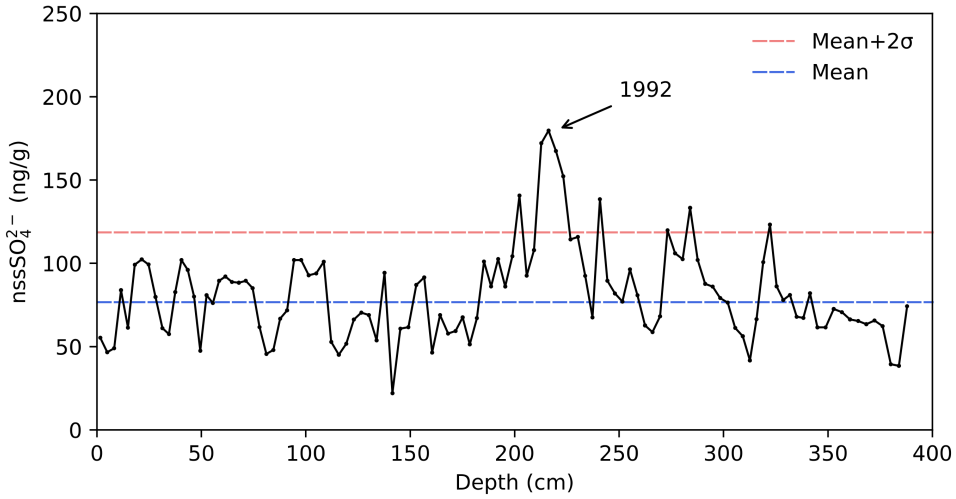

Figure 3. nss-sulphate concentration vs. depth profiles and dating of the Mount Pinatubo eruption. The dashed blue line represents the threshold for the biogenic background contribution to $nssSO_4^{2-}$. The dashed red line shows the mean +2σ for distinguishing the superimposed volcanic peak.

In the snow pit analyzed in this work, the highest $nssSO_4^{2-}$ concentration peak at about 200 cm depth is superimposed to the background (Figure 3).

The decisive assignment of the volcanic event was possible distinguishing this latter from the non-volcanic contribution to sulphate, that is, biogenic sulphate emission. For this assessment, we used the method described in [37,38]: firstly, the mean + 2σ was calculated along all the snow pit depth. From this calculation, the sample points which exceeded this threshold were temporarily discharged. Successively from the new data set, we calculated again the mean + 2σ. This second mean + 2σ is shown in Figure 3 by mean of the dashed red line. The four points that exceeded this threshold could be unequivocally considered as volcanic eruption. In particular, it was assigned the eruption of Mount Pinatubo, which happened in 1992.

However, it was not possible to find any trace of raising sulphate concentration due to the aerosol released from the Indonesian 1964 eruption, because the depth of the snow pit could not cover this time period. According to previous samplings, the lack of this peak was indeed expected for the depth of the snow pit.

We calculated the volcanic flux on the unique event identified using the method indicated in [38,39], obtaining a flux of 10.9 kg km^{-2}. This value perfectly agrees with the one found in [38].

According to this attribution, the annual accumulation rate for the period 1992–2016 could then be estimated in 9 cm snow yr^{-1}, quite in agreement with previous evaluations [11], which however covered a shorter time period.

Although an accurate assessment of the accumulation rate at yearly resolution is not possible given the presence of only one temporal horizon (two in the previous samplings) in the analyzed time frame, it is reasonable to deduce from the obtained results that the average accumulation rate has not changed significantly over the last decade (not covered by the previous snow pits), and this is quite relevant information in the framework of snow deposition and surface mass balance of the East Antarctic ice sheet.

4.3. Primary Aerosol

Figure 4 reports the stratigraphic records of the elements belonging to primary aerosol (sea salt and crustal) analyzed with both IC and ICP-OES techniques. The solid grey lines show the data sets obtained with IC analysis, while the crosses represent the elements analyzed by ICP-OES.

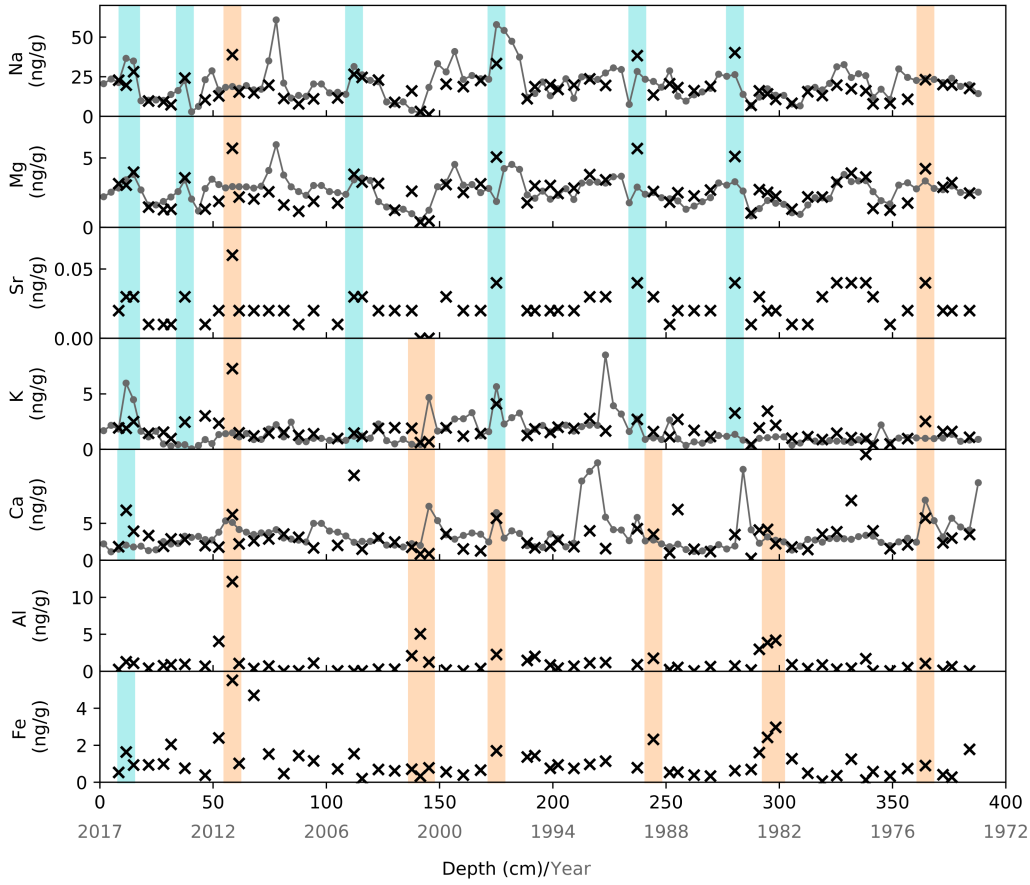

Figure 4. Concentration vs. depth profiles of (in order from top to bottom): Na, Mg, Sr, K, Ca, Al and Fe. Light blue stripes highlight recurrent peaks in the marine markers, while the light red stripes indicate recurrent peaks in the crustal markers. The solid lines specify the ions analyzed by IC, while the crosses indicate the elements analyzed by ICP-OES. The dating attributing is shown in the x label in grey.

The profiles of these elements exhibit a similar general trend, without an evident increasing or decreasing tendency during the studied interval span.

As already discussed above, sodium (with its extremely high percentage of sea salt origins), is considered as the most reliable marker for the sea spray, compared to the other marine markers [32].

Other ions such as Cl^-, Mg^{2+}, K^+, and Ca^{2+} are also present in significant amount in the total sea salt aerosol budget; however, chloride has important alternative sources and, moreover, is marked by post-depositional processes, affecting its concentration along the snow pit depth (for this reason, chloride will be separately discussed in Section 4.4) and potassium, magnesium, and calcium can be significantly affected by crustal inputs, depending on the elevation and distance from the coastline of the sampling site [40,41].

Previous studies [42–44] show that Sr is an element which mainly derives from sea salt aerosol; indeed, Na, Mg, and Sr (Figure 4) show extremely similar profiles with many in-phase concentration spikes, highlighted with light blue stripes, which are likely related to intense sea storm events. High-resolution aerosol measurements showed that these events mainly occur during winter (April–November), supplying relevant amounts of sea salt to inner plateau [30].

The other source of Mg and Sr besides sea salt, which is mainly crustal input that can reach the Dome C site together with marine air masses [43,45], is equally visible. A marked evidence is visible in the extremely high peak at 60 cm (Figure 4), which is clearly a crustal event which arrived in Dome C around 2011. Another less pronounced crustal event is around 360 cm. In this case, it was more likely a mixed supply, with both marine and crustal

contributions. Grotti et al. [43], in superficial snow samples collected in the same site, found extremely low concentrations of Sr and estimate its crustal contribution to be less than 20% of the total Sr on average. These results are in line with a study conducted on 37 sections of the Vostok ice core, in which Sr resulted dominated by crustal dust only during glacial periods, while other natural sources are more relevant during warmer periods [44].

Al, Fe, and Ca are the most important crustal constituents of atmospheric aerosol. Apart from water-insoluble mineral dust particles [5,46,47], Ca^{2+} ion is usually taken as the reference chemical marker for continental dust in Antarctic aerosol and snow, as it is easier to be determined than Al and Fe, especially in the internal regions, where sea spray contribution is low and continental long-range transport prevails on the Ca budget [15].

Al is considered one of the most reliable elements for representing the crustal sources, as it is one of the major constituents of the Earth's crust [48].

Polar ice cores preserve continuous, undisturbed and detailed stratigraphic records of mineral dust, from Multisizer Coulter Counter measurements, that can be used as proxies for paleoclimate and paleowinds [5]. In fact, Al is an excellent mineral dust proxy, but due to difficulty of determination (low concentration and complexity of methodologies), only few studies on Al in deep ice core are performed, highlighting the different dust load in glacial and interglacial periods. Legrand and Delmas's study [26] found a great difference between glacial and interglacial composition of Al (up to a factor of 27). Such difference is greater in the inner plateau, e.g., Vostok and Dome C, than in low-elevation sites. Similar results were found from studies separately considering the Vostok ice core [49] and EPICA ice core in Dome C [50].

In the latter work, the study was addressed also to Fe, which is an equally important element arising from aeolian dust transport from deserts inside continents [51]; moreover, in its soluble form, it influences many biogeochemical processes through fertilization processes over the oceanic region [52]. For these reasons, the capability to have a high-resolution record on Fe deserves a great importance.

In Dome C, several studies are available on this element in snow pits (e.g., [53]), superficial snow samples (e.g., [25,43]), and ice cores (e.g., [50,52]) but due to its importance in biogeochemical cycles it needs further investigations.

As shown in the Figure 4, Fe presents some similarities with the total dissolved Fe stratigraphy presented in [53], in particular, the highest peak at 60 cm in our snow pit corresponds to the highest peak found at around 30 cm in Burgay's study [53]. The different depth is due to the different time of snow pit dug (2017 and 2014 for our snow pit and the Burgay's work, respectively). The strong crustal-origin event occurred around 2011, which also influenced those typically marine elements and could be due to two different events. On the one hand, it could be related to the Puyehue-Cordón Caulle (Chile) volcanic eruption, which started in June 2011 and reached Antarctica around July 2011, as visible from satellite observations [54]. However, unlike the study conducted in West Antarctica, sulphate, which is more specific for describing a volcanic event, does not undergo a significant increase in this work compared to the background. On the other hand, it could be more likely related to the impact of the so-called La Niña event, which developed in the east Pacific from 2010–2011. From satellite and direct observations, La Niña resulted to be the strongest El Niño Southern Oscillation (ENSO) cold event in the past eight decades [55], which may have caused an extraordinary transport of mineral dust to Dome C site.

Concentration vs. depth profile of Fe exhibits the greatest similarities with Al. From previous studies, a general decreasing of concentration of these elements was found during the aerosol transport from coast to inland, but their principal source results unaltered [43]. A study carried out in the Mount Johns ice core site in West Antarctica found that Fe, interestingly, had a double origin: marine and crustal [17]; on the other hand, in Dome C, the strong correlation between Fe and Al (slope = 0.35, Pearson's r = 0.66, $p < 0.01$) seems to push in favor of the crustal origin alone, since their ratio is similar to the typical ratio found in the upper continental crust [56].

Unlike the other elements, the K^+ profile seems to not have a predominant source. Indeed, it shows evident different patterns, resulting in similarities with both the marine and crustal markers (Figure 4).

4.4. Post-Depositional Effects

Species that can be present in the atmosphere in the gas phase exhibit complexities concerning the interpretation of their records after deposition/absorption onto the ice sheets because of the strong interaction between ice and atmosphere. Post-depositional effects (e.g., desorption, diffusion, migration, chemical, and photochemical reactions) can occur and alter the actual air-to-snow transfer function, inferring paleo-climatic information. Some ice cores studies carried out in Antarctica [57] showed that, in general, concentration vs. depth profiles of species such as Cl^-, F^-, and $NO_3{}^-$ exhibited a rapid decrease in the first few meters, indicating that a fraction, sometimes major, of these compounds can form volatile acids in acidic snow layers, which were expelled back in the atmosphere after deposition [11,57], despite some redeposition processes of the gases which can occur in the upper firn layers due to its extremely low temperature. Surprisingly, a similar effect was found for methanesulfonic acid (MSA) [11] that is not as volatile as HNO_3 or HCl. The explanation for these post-depositional effects is related to the low snow accumulation rate allowing the snow surface to remain in contact with the atmosphere and solar radiation for long time after deposition; thus, snow/atmosphere exchanges processes of gaseous species after snow deposition are more likely to occur.

Figure 5 shows the gradual decreasing concentration trend of chloride, MSA, and nitrate as function of depth.

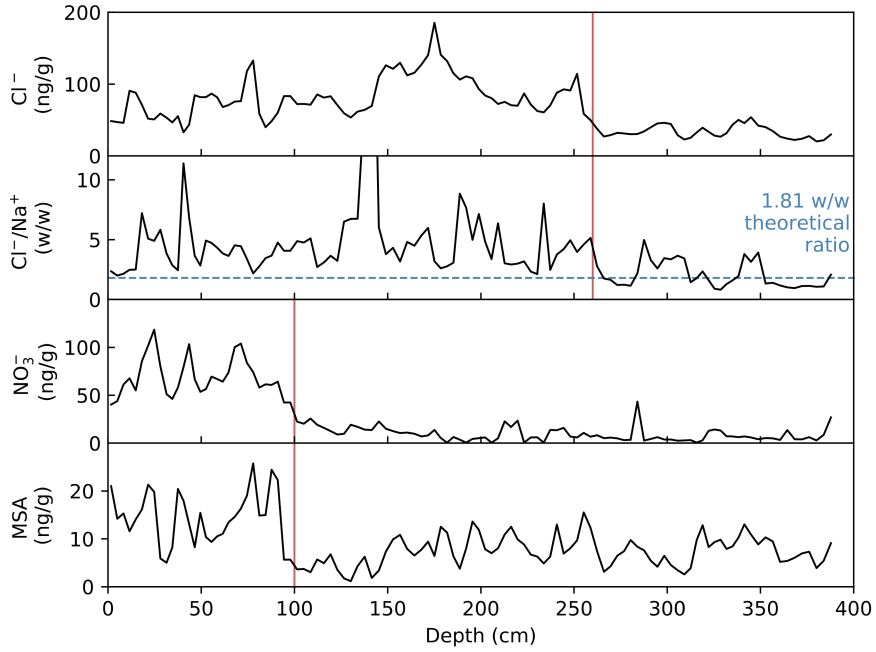

Figure 5. Concentration vs. depth of profile of the ions involved in post-depositional processes: Cl^-, $NO_3{}^-$ and MSA, and Cl^-/Na^+ ratio. The red vertical lines show the threshold of the post-depositional processes for the four ions.

Chloride in central Antarctic plateau arises from sea salt aerosol, but in the snow layer it is not correlated with Na [58]. This is due to the exchange reaction between the NaCl in the sea salt aerosol and the acidic species (mainly H_2SO_4 and HNO_3) forming volatile HCl [11,59]. Such reactions take place in the atmosphere during the transport and are more evident in the aged aerosol than in freshly formed sea spray. This aerosol fractionating effect, occurring during transport from the sea to the sampling site, leads to the loss of

chloride with respect to typical sea salt composition (chloride depletion). As a result, the gaseous HCl formed from sea spray is deposited in the same way as gaseous HNO_3 on the superficial snow layer in the low accumulation site due to the extremely low temperature and high superficial areas of icy crystal of the snow, acting as cold condenser for gaseous species. In this way on the superficial snow layers, chloride concentrations are higher than expected, and the Cl^-/Na^+ ratio is higher than the sea water ratio (Figure 5). As it is possible to see in Figure 5, Cl^-/Na^+ ratio is extremely high in comparison to the theoretical seawater ratio (1.81 w/w) in the first 2.6 m; after this depth, the ratio becomes lower until it settles down to a value of 1 under 3.5 m.

When Cl^- exceeds the Cl^-/Na^+ ratio in sea water, especially in the most superficial snow layers, it means that extra sources for Cl^- are not negligible, mostly from the presence of long-range transport mechanisms [11].

The deposition of HCl is reversible due to temperature variations of superficial snow and winds allowing modification of icy crystal that, due to the vary low accumulation rate, remain for a long time in contact with the atmosphere, which allows the HCl to be re-emitted into the atmosphere.

Nitrate is one of the main components in Antarctic deposition. The extent and exact timing of possible nitrate sources is still open to debate, but the in-phase relationship found with the UV solar flux both for aerosol and surface snow suggests a relevant role of solar irradiance both in the UV photolysis [60,61] and also in subsequent oxidation of NO_x and/or the presence of a major nitrate source [62].

Nitrate concentration vs. depth profile at Dome C shows a marked decreasing trend, which is extremely sharp in the first meter of depth (Figure 5). In fact, the superficial concentration values fall abruptly from a spike of 120 ng g^{-1} in the first meter of depth to a background level of about 9 ng g^{-1} in the deeper layers. This result is in agreement with the one achieved by [11], which reports a loss of about 90% of nitrate already in the first m depth. In our study, we observed a drop of about 87% from the uppermost layers.

In spite of this substantial loss as depth increases, concentration peaks superimposed to the (much lower) background can still be observed, for instance in the case of the small peak around 210 m depth, which corresponds to the concurrent deposition of Pinatubo volcanic aerosol. Indeed, some works identified reactive nitrogen species in near-source plumes from open-vent sources (e.g., [63]), including species such as nitrogen oxides (NO_x) and nitric acid, mostly in the gas phase. Thermal volcanic nitrogen fixation is thought to occur due to the elevated temperatures at volcanic vents [64].

As concerning MSA, it originates only from the atmospheric oxidation of dimethyl sulfide (DMS), therefore its biological marine source is indisputable. MSA records from Antarctic ice cores are considered useful for reconstructing the history of Southern Ocean biological productivity, also controlled by atmosphere/ocean teleconnections (e.g., El Niño-like phenomena), and past sea ice extent [65–67]. However, the extraction of climatic and environmental information from such records is complicated by the post-depositional processes affecting MSA, as it was seen in several Antarctic sites [68].

Figure 5 also shows the plot of MSA concentration as a function of the depth. As previously observed for chloride and nitrate, concentration decreases as depth increases. In fact, it is possible to appreciate the drop from an average value of about 15 ng/g in the top meter depth of the snow pit to one of about 7.5 ng/g as background average in the samples deeper than 1 m. Quantifying MSA losses is not straightforward due to the pluri-annual oscillation pattern that is superimposed on the decreasing trend of background values [11]. Nevertheless, given the considerable depth of the snow pit and the availability of a large number of data, we can attempt an evaluation of the extent of the post-depositional processes affecting MSA at Dome C site, corresponding to a loss of about 50% from the shallowest to the deeper (than 1 m) layers. Although the shape of the decreasing trend is quite similar to the one of nitrate more than chloride (exhibiting a more gradual behavior), the extent of loss is definitely lower.

By considering all these results together, we can observe a similar behavior for MSA and nitrate, both showing sudden decreases more or less around 1 m depth while a much more gradual decreasing pattern is evident for chloride, showing a rather constant decrease in the shallowest 2.5 m. Therefore, 1 m and 2.5 m can be taken as depth thresholds for the occurrence and completion of the post-depositional process for the three components. The estimation of such a threshold for chloride is confirmed by the trend of Cl^-/Na^+ ratio (Figure 5), showing a quite constant value in the top 2.5 m (average value 4.90 $\pm$ 4.1) and another relatively constant but lower value in the samples deeper than 2.5 m (average value 2.2 $\pm$ 1.2), which is definitely comparable with the sea water ratio.

This difference can be due to the different mobility (diffusion) of the corresponding acidic species (HNO_3, CH_3SO_3H and HCl), which are likely the ones who are mobilized through different acidic snow layers [57].

5. Conclusions

The chemical characterizations of the atmospheric depositions during the last decades confirmed the results from previous studies in the same site, expanding the investigated period. Moreover, it was possible to obtain, for the first time, a record of major elements in snow pit samples by ICP-OES, despite their low concentrations.

Comparison of IC and ICP-OES data indicated that for K, Ca, and, partly, Mg, the ICP-OES technique can also determine insoluble particles, which are not detectable by IC, providing complementary information. Instead, the two techniques seemed to be equivalent concerning sodium.

Sample dating by $nssSO_4^{2-}$ measurements allowed for evaluation at an accumulation rate of 9 cm snow yr^{-1}, confirming the suitability of the Dome C site for the ice core drilling and the evaluation of past climatic variations.

The high percentages of sea salt sodium and non-sea salt calcium made possible to conclude that their extra sources are almost negligible, making them eligible as reliable markers for sea salt and crust, respectively. In addition to sodium, although extra sources are relevant, Mg and Sr markedly resulted to arise from marine sources, whereas, together with calcium, Al and Fe originated from crustal inputs. In particular, the crustal event, which involved almost all the elements analyzed around 2011, could be due to the Puyehue-Cordón Caulle (Chile) volcanic eruption, which occurred in June 2011 and arrived in Antarctica in July 2011, or, more likely, to the La-Niña event, which was the strongest ENSO cold event of the last eight decades. Further investigations will be needed to better understand this interesting event.

In parallel, post-depositional effects on species, such as nitrate, MSA, and chloride, were investigated, finding such effects to conclude at a threshold of 1 m for NO_3^- and MSA and of 2.5 m for Cl^-.

Supplementary Materials: The following are available online at https://www.mdpi.com/article/10.3390/atmos12070909/s1.

Author Contributions: Conceptualization, L.C., S.B. (Silvia Becagli), S.B. (Stefano Bertinetti), R.T. and S.N.; methodology, M.S., S.B. (Stefano Bertinetti), R.T., M.G. and L.C.; validation, M.S., S.B. (Stefano Bertinetti), R.T. and M.G.; formal analysis, L.C., S.B. (Stefano Bertinetti) and M.S.; investigation, R.T., L.C., S.B. (Stefano Bertinetti) and M.G.; resources, R.T., M.G. and S.N.; writing—original draft preparation, L.C., S.B. (Stefano Bertinetti) and R.T.; writing—review and editing, S.B. (Silvia Becagli) and S.N.; visualization, L.C.; supervision, S.N. and R.T.; project administration, S.N.; funding acquisition, S.N. All authors have read and agreed to the published version of the manuscript.

Funding: The research was financially supported by the MIUR (Italian Ministry of University and Research) and PNRA (Programma Nazionale di Ricerca in Antartide) through the PNRA 2016/AC2.04 (PNRA 16_00252-Linea A2) Project "SIDDARTA: Source IDentification of (mineral) Dust to AntaRcTicA" and PNRA 2015/AC3.04 (PNRA 14_00091-Linea A3) Project "LTCPAA: Long-Term Measurements of Chemical and Physical Properties of Atmospheric Aerosol at Dome C".

Institutional Review Board Statement: Not applicable.

Informed Consent Statement: Not applicable.

Data Availability Statement: Data are available upon request to the authors.

Acknowledgments: We want to thank all the researchers who helped us to dig by hand the snow pit and collect the samples and the PNRA ((Programma Nazionale di Ricerca in Antartide) logistic staff, who supported this activity.

Conflicts of Interest: The authors declare no conflict of interest. The funders had no role in the design of the study, in the collection, analyses, or interpretation of data in the writing of the manuscript, or in the decision to publish the results.

References

1. EPICA Community Members. Eight glacial cycles from an Antarctic ice core. *Nature* **2004**, *429*, 623–628. [CrossRef] [PubMed]
2. EPICA Community Members; Barbante, C.; Barnola, J.-M.; Becagli, S.; Beer, J.; Bigler, M.; Boutron, C.; Blunier, T.; Castellano, E.; Cattani, O.; et al. One-to-one coupling of glacial climate variability in Greenland and Antarctica. *Nat. Cell Biol.* **2006**, *444*, 195–198. [CrossRef]
3. Wolff, E.; Barbante, C.; Becagli, S.; Bigler, M.; Boutron, C.; Castellano, E.; de Angelis, M.; Federer, U.; Fischer, H.; Fundel, F.; et al. Changes in environment over the last 800,000 years from chemical analysis of the EPICA Dome C ice core. *Quat. Sci. Rev.* **2010**, *29*, 285–295. [CrossRef]
4. Abram, N.; Wolff, E.; Curran, M.A. A review of sea ice proxy information from polar ice cores. *Quat. Sci. Rev.* **2013**, *79*, 168–183. [CrossRef]
5. Delmonte, B.; Petit, J.R.; Maggi, V. Glacial to Holocene implications of the new 27000-year dust record from the EPICA Dome C (East Antarctica) ice core. *Clim. Dyn.* **2002**, *18*, 647–660.
6. Traversi, R.; Usoskin, I.G.; Solanki, S.; Becagli, S.; Frezzotti, M.; Severi, M.; Stenni, B.; Udisti, R. Nitrate in Polar Ice: A New Tracer of Solar Variability. *Sol. Phys.* **2012**, *280*, 237–254. [CrossRef]
7. Genthon, C.; Six, D.; Scarchilli, C.; Ciardini, V.; Frezzotti, M. Meteorological and snow accumulation gradients across Dome C, East Antarctic plateau. *Int. J. Clim.* **2015**, *36*, 455–466. [CrossRef]
8. Petit, J.R.; Jouzel, J.; Pourchet, M.; Merlivat, L. A detailed study of snow accumulation and stable isotope content in Dome C (Antarctica). *J. Geophys. Res. Space Phys.* **1982**, *87*, 4301–4308. [CrossRef]
9. Fischer, H.; Fundel, F.; Ruth, U.; Twarloh, B.; Wegner, A.; Udisti, R.; Becagli, S.; Castellano, E.; Morganti, A.; Severi, M.; et al. Reconstruction of millennial changes in dust emission, transport and regional sea ice coverage using the deep EPICA ice cores from the Atlantic and Indian Ocean sector of Antarctica. *Earth Planet. Sci. Lett.* **2007**, *260*, 340–354. [CrossRef]
10. Parrenin, F.; Cavitte, M.G.P.; Blankenship, D.D.; Chappellaz, J.; Fischer, H.; Gagliardini, O.; Masson-Delmotte, V.; Passalacqua, O.; Ritz, C.; Roberts, J.; et al. Is there 1.5-million-year-old ice near Dome C, Antarctica? *Cryosphere* **2017**, *11*, 2427–2437. [CrossRef]
11. Traversi, R.; Becagli, S.; Castellano, E.; Cerri, O.; Morganti, A.; Severi, M.; Udisti, R. Study of Dome C site (East Antartica) variability by comparing chemical stratigraphies. *Microchem. J.* **2009**, *92*, 7–14. [CrossRef]
12. Legrand, M.; Mayewski, P. Glaciochemistry of polar ice cores: A review. *Rev. Geophys.* **1997**, *35*, 219–243. [CrossRef]
13. Legrand, M.; Wolff, E.; Wagenbach, D. Antarctic aerosol and snowfall chemistry: Implications for deep Antarctic ice-core chemistry. *Ann. Glaciol.* **1999**, *29*, 66–72. [CrossRef]
14. Kekonen, T.; Perämäki, P.; Moore, J. Comparison of analytical results for chloride, sulfate and nitrate obtained from adjacent ice core samples by two ion chromatographic methods. *J. Environ. Monit.* **2004**, *6*, 147–152. [CrossRef]
15. Morganti, A.; Becagli, S.; Castellano, E.; Severi, M.; Traversi, R.; Udisti, R. An improved flow analysis–ion chromatography method for determination of cationic and anionic species at trace levels in Antarctic ice cores. *Anal. Chim. Acta* **2007**, *603*, 190–198. [CrossRef]
16. Liu, K.; Hou, S.; Wu, S.; Zhang, W.; Zou, X.; Yu, J.; Song, J.; Sun, X.; Huang, R.; Pang, H.; et al. Assessment of heavy metal contamination in the atmospheric deposition during 1950–2016 A.D. from a snow pit at Dome A, East Antarctica. *Environ. Pollut.* **2021**, *268*, 115848. [CrossRef]
17. Schwanck, F.; Simões, J.C.; Handley, M.; Mayewski, P.A.; Auger, J.D.; Bernardo, R.T.; Aquino, F.E. A 125-year record of climate and chemistry variability at the Pine Island Glacier ice divide, Antarctica. *Cryosphere* **2017**, *11*, 1537–1552. [CrossRef]
18. Bertinetti, S.; Ardini, F.; Caiazzo, L.; Grotti, M. Determination of major elements in Antarctic snow by inductively coupled plasma optical emission spectrometry using a total-consumption sample introduction system. *Spectrochim. Acta Part B Spectrosc.* **2021**, *181*, 106231. [CrossRef]
19. Urbini, S.; Frezzotti, M.; Gandolfi, S.; Vincent, C.; Scarchilli, C.; Vittuari, L.; Fily, M. Historical behaviour of Dome C and Talos Dome (East Antarctica) as investigated by snow accumulation and ice velocity measurements. *Glob. Planet. Chang.* **2008**, *60*, 576–588. [CrossRef]
20. Bertinetti, S.; Ardini, F.; Vecchio, M.A.; Caiazzo, L.; Grotti, M. Isotopic analysis of snow from Dome C indicates changes in the source of atmospheric lead over the last fifty years in East Antarctica. *Chemosphere* **2020**, *255*, 126858. [CrossRef]

21. Caiazzo, L.; Becagli, S.; Frosini, D.; Giardi, F.; Severi, M.; Traversi, R.; Udisti, R. Spatial and temporal variability of snow chemical composition and accumulation rate at Talos Dome site (East Antarctica). *Sci. Total. Environ.* **2016**, *550*, 418–430. [CrossRef] [PubMed]
22. Grotti, M.; Soggia, F.; Todolì, J.L. Ultratrace analysis of Antarctic snow samples by reaction cell inductively coupled plasma mass spectrometry using a total-consumption micro-sample-introduction system. *Analyst* **2008**, *133*, 1388–1394. [CrossRef] [PubMed]
23. Paredes, E.; Grotti, M.; Mermet, J.M.; Todolí, J.L. Heated-spray chamber-based low sample consumption system for inductively coupled plasma spectrometry. *J. Anal. Spectrom.* **2009**, *24*, 903–910. [CrossRef]
24. Grotti, M.; Ardini, F.; Todolì, J.L. Total introduction of microsamples in inductively coupled plasma mass spectrometry by high-temperature evaporation chamber with a sheathing gas stream. *Anal. Chim. Acta* **2013**, *767*, 14–20. [CrossRef]
25. Grotti, M.; Soggia, F.; Ardini, F.; Magi, E.; Becagli, S.; Traversi, R.; Udisti, R. Year-round record of dissolved and particulate metals in surface snow at Dome Concordia (East Antarctica). *Chemosphere* **2015**, *138*, 916–923. [CrossRef]
26. Legrand, M.; Delmas, R.J. Soluble impurities in four Antarctic ice cores over the last 30,000 years. *Ann. Glaciol.* **1988**, *10*, 116–120. [CrossRef]
27. Röthlisberger, R.; Mulvaney, R.; Wolff, E.; Hutterli, M.A.; Bigler, M.; Sommer, S.; Jouzel, J. Dust and sea salt variability in central East Antarctica (Dome C) over the last 45 kyrs and its implications for southern high-latitude climate. *Geophys. Res. Lett.* **2002**, *29*, 24-1–24-4. [CrossRef]
28. Bowen, H.J.M. *Environmental Chemistry of the Elements*; Academic Press: London, UK, 1979.
29. Nozaki, Y. A Fresh Look at Element Distribution in the North Pacific. EOS, American Geophysical Union. 1997. Available online: http://www.agu.org/eos_elec/97025e.html (accessed on 22 June 2021).
30. Udisti, R.; Dayan, U.; Becagli, S.; Busetto, M.; Frosini, D.; Legrand, M.; Lucarelli, F.; Preunkert, S.; Severi, M.; Traversi, R.; et al. Sea spray aerosol in central Antarctica. Present atmospheric behaviour and implications for paleoclimatic reconstructions. *Atmos. Environ.* **2012**, *52*, 109–120. [CrossRef]
31. Piccardi, G.; Becagli, S.; Traversi, R.; Udisti, R. Fractionating phenomena. altitude induced, on snow composition in Northern Victoria Land (Antarctica). *Ital. Res. Antarct. Atmos.* **1996**, *51*, 229–245.
32. Wolff, E.W.; Rankin, A.M.; Röthlisberger, R. An ice core indicator of Antarctic sea ice production? *Geophys. Res. Lett.* **2003**, *30*, 2158. [CrossRef]
33. Becagli, S.; Proposito, M.; Benassai, S.; Gragnani, R.; Magand, O.; Traversi, R.; Udisti, R. Spatial distribution of biogenic sulphur compounds (MSA, nssSO_4 2–) in the northern Victoria Land–Dome C–Wilkes Land area, East Antarctica. *Ann. Glaciol.* **2005**, *41*, 23–31. [CrossRef]
34. Bertler, N.; Mayewski, P.A.; Aristarain, A.; Barrett, P.; Becagli, S.; Bernardo, R.; Bo, S.; Xiao, C.; Curran, M.; Qin, D.; et al. Snow chemistry across Antarctica. *Ann. Glaciol.* **2005**, *41*, 167–179. [CrossRef]
35. Hammer, C.U.; Clausen, H.B.; Dansgaard, W.; Gundestrup, N.; Johnsen, S.J.; Reeh, N. Dating of Greenland ice cores by flow models, isotopes, volcanic debris, and continental dust. *J. Glaciol.* **1978**, *20*, 82. [CrossRef]
36. Delmas, R.J.; Legrand, M.; Aristarain, A.J.; Zanolini, F. Volcanic deposits in Antarctic snow and ice. *J. Geophys. Res. Space Phys.* **1985**, *90*, 12901. [CrossRef]
37. Cole-Dai, J.; Mosley-Thompson, E. The Pinatubo eruption in South Pole snow and its potential value to ice-core paleovolcanic records. *Ann. Glaciol.* **1999**, *29*, 99–105. [CrossRef]
38. Castellano, E.; Becagli, S.; Hansson, M.; Hutterli, M.; Petit, J.R.; Rampino, M.R.; Severi, M.; Steffensen, J.P.; Traversi, R.; Udisti, R. Holocene volcanic history as recorded in the sulfate stratigraphy of the European Project for Ice Coring in Antarctica Dome C (EDC96) ice core. *J. Geophys. Res. Space Phys.* **2005**, *110*, 110. [CrossRef]
39. Nardin, R.; Amore, A.; Becagli, S.; Caiazzo, L.; Frezzotti, M.; Severi, M.; Stenni, B.; Traversi, R. Volcanic Fluxes Over the Last Millennium as Recorded in the Gv7 Ice Core (Northern Victoria Land, Antarctica). *Geosciences* **2020**, *10*, 38. [CrossRef]
40. Benassai, S.; Becagli, S.; Gragnani, R.; Magand, O.; Proposito, M.; Fattori, I.; Traversi, R.; Udisti, R. Sea-spray deposition in Antarctic coastal and plateau areas from ITASE traverses. *Ann. Glaciol.* **2005**, *41*, 32–40. [CrossRef]
41. Traversi, R.; Becagli, S.; Castellano, E.; Largiuni, O.; Migliori, A.; Severi, M.; Frezzotti, M.; Udisti, R. Spatial and temporal distribution of environmental markers from Coastal to Plateau areas in Antarctica by firn core chemical analysis. *Int. J. Environ. Anal. Chem.* **2004**, *84*, 457–470. [CrossRef]
42. Tuohy, A.; Bertler, N.; Neff, P.; Edwards, R.; Emanuelsson, D.; Beers, T.; Mayewski, P. Transport and deposition of heavy metals in the Ross Sea Region, Antarctica. *J. Geophys. Res. Atmos.* **2015**, *120*, 120. [CrossRef]
43. Grotti, M.; Soggia, F.; Ardini, F.; Magi, E.; Grotti, M.; Soggia, F.; Ardini, F.; Magi, E. Major and trace element partitioning between dissolved and particulate phases in Antarctic surface snow. *J. Environ. Monit.* **2011**, *13*, 2511–2520. [CrossRef]
44. Gabrielli, P.; Planchon, F.; Hong, S.; Lee, K.H.; Hur, S.D.; Barbante, C.; Ferrari, C.P.; Petit, J.R.; Lipenkov, V.; Cescon, P. Trace elements in Vostok Antarctic ice during the last four climatic cycles. *Earth Planet. Sci. Lett.* **2005**, *234*, 249–259. [CrossRef]
45. Becagli, S.; Proposito, M.; Benassai, S.; Flora, O.; Genoni, L.; Gragnani, R.; Largiuni, O.; Pili, S.L.; Severi, M.; Stenni, B.; et al. Chemical and isotopic snow variability in East Antarctica along the 2001/02 ITASE traverse. *Ann. Glaciol.* **2004**, *39*, 473–482. [CrossRef]
46. Lambert, F.R.; Delmonte, B.; Petit, J.-R.; Bigler, M.; Kaufmann, P.R.; Hutterli, M.A.; Stocker, T.F.; Ruth, U.; Steffensen, J.P.; Maggi, V. Dust-climate couplings over the past 800,000 years from the EPICA Dome C ice core. *Nature* **2008**, *452*, 616–619. [CrossRef]

47. Marino, F.; Castellano, E.; Nava, S.; Chiari, M.; Ruth, U.; Wegner, A.; Lucarelli, F.; Udisti, R.; Delmonte, B.; Maggi, V. Coherent composition of glacial dust on opposite sides of the East Antarctic Plateau inferred from the deep EPICA ice cores. *Geophys. Res. Lett.* **2009**, *36*, 23703. [CrossRef]
48. Planchon, F.A.; Boutron, C.F.; Barbante, C.; Cozzi, G.; Gaspari, V.; Wolff, E.; Ferrari, C.P.; Cescon, P. Changes in heavy metals in Antarctic snow from Coats Land since the mid-19th to the late-20th century. *Earth Planet. Sci. Lett.* **2002**, *200*, 207–222. [CrossRef]
49. De Angelis, M.; Legrand, M.; Petit, J.R.; Barkov, N.I.; Korotkevitch, Y.S.; Kotlyakov, V.M. Soluble and insoluble impurities along the 950 m deep Vostok ice core (Antarctica)—Climatic implications. *J. Atmos. Chem.* **1983**, *1*, 215–239. [CrossRef]
50. Traversi, R.; Barbante, C.; Gaspari, V.; Fattori, I.; Largiuni, O.; Magaldi, L.; Udisti, R. Aluminium and iron record for the last 28 kyr derived from the Antarctic EDC96 ice core using new CFA methods. *Ann. Glaciol.* **2004**, *39*, 300–306. [CrossRef]
51. Jickells, T.D.; Anderson, K.; Andersen, K.K.; Baker, A.R.; Bergametti, G.; Brooks, N.; Cao, J.J.; Boyd, P.; Duce, R.A.; Hunter, K.A.; et al. Global Iron Connections Between Desert Dust, Ocean Biogeochemistry, and Climate. *Science* **2005**, *308*, 67–71. [CrossRef]
52. Conway, T.; Wolff, E.; Röthlisberger, R.; Mulvaney, R.; Elderfield, H. Constraints on soluble aerosol iron flux to the Southern Ocean at the Last Glacial Maximum. *Nat. Commun.* **2015**, *6*, 7850. [CrossRef]
53. Burgay, F.; Barbaro, E.; Cappelletti, D.; Turetta, C.; Gallet, J.-C.; Isaksson, E.; Stenni, B.; Dreossi, G.; Scoto, F.; Barbante, C.; et al. First discrete iron(II) records from Dome C (Antarctica) and the Holtedahlfonna glacier (Svalbard). *Chemosphere* **2021**, *267*, 129335. [CrossRef] [PubMed]
54. Koffman, B.G.; Dowd, E.G.; Osterberg, E.C.; Ferris, D.; Hartman, L.H.; Wheatley, S.D.; Kurbatov, A.V.; Wong, G.J.; Markle, B.; Dunbar, N.W.; et al. Rapid transport of ash and sulfate from the 2011 Puyehue-Cordón Caulle (Chile) eruption to West Antarctica. *J. Geophys. Res. Atmos.* **2017**, *122*, 8908–8920. [CrossRef]
55. Boening, C.; Willis, J.K.; Landerer, F.W.; Nerem, R.S.; Fasullo, J. The 2011 La Niña: So strong, the oceans fell. *Geophys. Res. Lett.* **2012**, *39*, 19602. [CrossRef]
56. Henderson, P.; Henderson, G.M. *The Cambridge Handbook of Earth Science Data*; Cambridge University Press: Cambridge, UK, 2009.
57. Wagnon, P.; Delmas, R.J.; Legrand, M.; Wagnon, P.; Delmas, R.J.; Legrand, M. Loss of volatile acid species from upper firn layers at Vostok, Antarctica. *J. Geophys. Res. Space Phys.* **1999**, *104*, 3423–3431. [CrossRef]
58. Wagenbach, D.; Ducroz, F.; Mulvaney, R.; Keck, L.; Minikin, A.; Legrand, M.; Hall, J.S.; Wolff, E.; Wagenbach, D.; Ducroz, F.; et al. Sea-salt aerosol in coastal Antarctic regions. *J. Geophys. Res. Space Phys.* **1998**, *103*, 10961–10974. [CrossRef]
59. Legrand, M.; Delmas, R. The ionic balance of Antarctic snow: A 10-year detailed record. *Atmos. Environ.* **1984**, *18*, 1867–1874. [CrossRef]
60. Grannas, A.M.; Jones, A.E.; Dibb, J.; Ammann, M.; Anastasio, C.; Beine, H.J.; Bergin, M.; Bottenheim, J.; Boxe, C.S.; Carver, G.; et al. An overview of snow photochemistry: Evidence, mechanisms and impacts. *Atmos. Chem. Phys. Discuss.* **2007**, *7*, 4329–4373. [CrossRef]
61. Röthlisberger, R.; Hutterli, M.A.; Wolff, E.; Mulvaney, R.; Fischer, H.; Bigler, M.; Goto-Azuma, K.; Hansson, M.E.; Ruth, U.; Siggaard-Andersen, M.-L.; et al. Nitrate in Greenland and Antarctic ice cores: A detailed description of post-depositional processes. *Ann. Glaciol.* **2002**, *35*, 209–216. [CrossRef]
62. Traversi, R.; Becagli, S.; Brogioni, M.; Caiazzo, L.; Ciardini, V.; Giardi, F.; Legrand, M.; Macelloni, G.; Petkov, B.; Preunkert, S.; et al. Multi-year record of atmospheric and snow surface nitrate in the central Antarctic plateau. *Chemosphere* **2017**, *172*, 341–354. [CrossRef]
63. Oppenheimer, C.; Kyle, P.; Tsanev, V.; Mcgonigle, A.; Mather, T.; Sweeney, D. Mt. Erebus, the largest point source of NO_2 in Antarctica. *Atmos. Environ.* **2005**, *39*, 6000–6006. [CrossRef]
64. Mather, T.A.; Pyle, D.M.; Allen, A.G. Volcanic source for fixed nitrogen in the early Earth's atmosphere. *Geology* **2004**, *32*, 905–908. [CrossRef]
65. Legrand, M.; Feniet-Saigne, C. Methanesulfonic acid in South polar snow layers: A record of strong El Niño? *Geophys. Res. Lett.* **1991**, *18*, 187–190. [CrossRef]
66. Becagli, S.; Castellano, E.; Cerri, O.; Curran, M.; Frezzotti, M.; Marino, F.; Morganti, A.; Proposito, M.; Severi, M.; Traversi, R.; et al. Methanesulphonic acid (MSA) stratigraphy from a Talos Dome ice core as a tool in depicting sea ice changes and southern atmospheric circulation over the previous 140 years. *Atmos. Environ.* **2009**, *43*, 1051–1058. [CrossRef]
67. Curran, M.A.J.; van Ommen, T.D.; Morgan, V.I.; Phillips, K.L.; Palmer, A.S. Ice Core Evidence for Antarctic Sea Ice Decline Since the 1950s. *Science* **2003**, *302*, 1203–1206. [CrossRef]
68. Weller, R.; Traufetter, F.; Fischer, H.; Oerter, H.; Piel, C.; Miller, H. Postdepositional losses of methane sulfonate, nitrate, and chloride at the European Project for Ice Coring in Antarctica deep-drilling site in Dronning Maud Land, Antarctica. *J. Geophys. Res. Space Phys.* **2004**, *109*. [CrossRef]

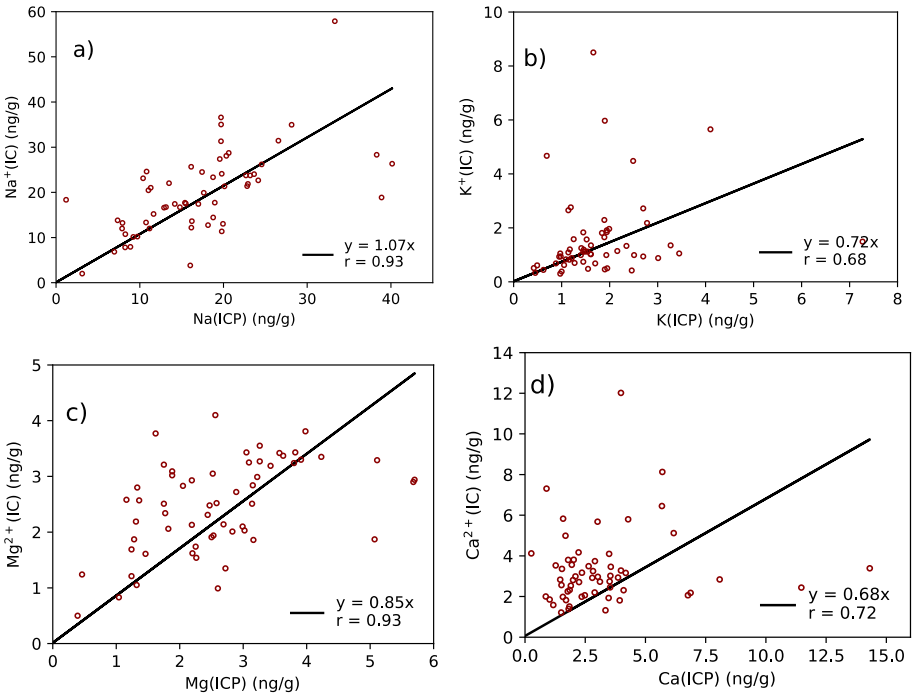

Figure S1. Scatter plots for Na vs. Na^+ (**a**), K vs. K^+ (**b**), Mg vs. Mg^{2+} (**c**) and Ca vs. Ca^{2+} (**d**) data. Regression line was forced through zero.